



Reaction-sintered porous mineral-based mullite ceramic membrane supports made from recycled materials

Yingchao Dong^{a,b,*}, Jian-er Zhou^a, Bin Lin^b, Yongqing Wang^a, Songlin Wang^b, Lifeng Miao^a, Ying Lang^a, Xingqin Liu^b, Guangyao Meng^b

^a Key Lab of Jiangxi Universities for Inorganic Membranes, National Engineering Research Center for Domestic and Building Ceramics, Jingdezhen Ceramic University (JCU), Jingdezhen, Jiangxi, 333001, PR China

^b USTC Lab for Solid State Chemistry and Inorganic Membranes, Department of Materials Science and Engineering, University of Science and Technology of China (USTC), Hefei, 230026, PR China

ARTICLE INFO

Article history:

Received 3 April 2009

Received in revised form 29 June 2009

Accepted 29 June 2009

Available online 4 July 2009

Keywords:

Membrane supports

Mullite

Self-expansion sintering

Fly ash

Waste recycling

ABSTRACT

Bulk porous mullite supports for ceramic membranes were prepared directly using a mixture of industrial waste fly ash and bauxite by dry-pressing, followed by sintering between 1200 and 1550 °C. The effects of sintering temperature on the phase composition and shrinkage percent of porous mullite were studied. The XRD results indicate that secondary mullitization reaction took place above 1200 °C, and completed at 1450 °C. During sintering, the mixture samples first shrunk, then expanded abnormally between 1326 and 1477 °C, and finally shrunk again above 1477 °C. This unique volume self-expansion is ascribed to the secondary mullitization reaction between bauxite and fly ash. More especially, the micro-structural variations induced by this self-expansion sintering were verified by SEM, porosity, pore size distribution and nitrogen gas permeation flux. During self-expansion sintering, with increasing temperature, an abnormal increase in both open porosity and pore size is observed, which also results in the increase of nitrogen gas flux. The mineral-based mullite supports with increased open porosity were obtained. Furthermore, the sintered porous mullite membrane supports were characterized in terms of thermal expansion co-efficient and mechanical strength.

© 2009 Elsevier B.V. All rights reserved.

1. Introduction

Nowadays, with strong environmental demands, porous ceramic membranes should be leading candidates for applications such as massive liquid waste pre-treatment, strong acidic or alkaline media separation and thermal shock separation applications, but they cannot be used on a large scale in industry due to their several drawbacks such as high cost, rare membrane materials and narrow application range. In recent years, porous mineral-based ceramic membranes have attracted much attention in the scientific community for their outstanding merits such as low cost, species diversity and novel additional properties [1–3]. Also, the development of novel porous mineral-based ceramics will lead to a critical new technological revolution that will add great economic value to natural minerals and to industrial waste materials, which exist widely throughout the world and many of which are not currently well utilized.

Generally, alumina is considered as starting material for the fabrication of porous ceramic supports for traditional ceramic separation membranes [4,5]. However, the application of macro-porous alumina supported ceramic membranes is greatly limited due to the high cost of both starting materials and sintering process. In recent years, some researchers have been devoted to develop new types of porous mineral-based ceramic membrane supports directly using abundant raw materials such as natural minerals and industrial wastes [6–11]. Mullite is the only stable crystalline aluminosilicate phase in the SiO₂–Al₂O₃ binary system [12]. The porous mullite materials exhibit many advantages such as low expansion co-efficient, good high-temperature strength and creep resistance, low density and good chemical inertness [13,14]. All of these characteristics make porous mullite be suitable to be widely applied as ceramic filters, catalyst or membrane supports and refractory bricks. Usually, industrial grade or chemical method derived powders are used for the preparation of porous mullite ceramics by the physical sintering technique. This method is at the cost of expensive starting materials, which are synthesized beforehand. Reaction sintering is a simple and cost-effective fabrication technique to produce porous mullite ceramics directly using some Al₂O₃–SiO₂ system industrial wastes or minerals. More especially, interestingly, porous micro-structure and targeted crystalline phase could

* Corresponding author at: Department of Materials Science and Engineering, University of Science and Technology of China (USTC), No. 96 Jinzhai Road, Hefei, Anhui Province, 230026, PR China. Tel.: +86 551 3606249; fax: +86 551 3607627.

E-mail address: dongyc9@mail.ustc.edu.cn (Y. Dong).

be effectively controlled during one-step reaction sintering process under suitable process conditions.

Fly ash is a by-product from the combustion of raw coal in thermal power plants. This industrial waste nowadays presents serious problems of storing and environmental pollution. Therefore, the effective utilization of waste fly ash not only decreases environmental pollution, but also produces high value-added products. In recent years, there have been a great deal of efforts made on preparing cordierite [15–18] and other glass–ceramics [19–23] from this industrial waste. In our previous work [24], dense mullite was synthesized from fly ash and bauxite mineral by dry-pressing. It was found that a unique volume self-expansion occurred before full densification during high-temperature sintering process. This self-expansion does not favor for the preparation of dense mullite ceramics. But for porous ceramics, volume expansion is expected to create a more porous micro-structure without pore-forming additive. Therefore, it is an interesting research topic to utilize this self-expansion to prepare reaction-sintered porous mullite from fly ash and bauxite.

In the current work, porous mineral-based mullite ceramic membrane supports were prepared through volume self-expansion by deliberate incomplete sintering densification directly using natural bauxite and industrial waste fly ash as the starting materials. The effect of sintering temperature on the properties of porous mullite was studied in detail, focused on phase composition, sintering shrinkage percent, pore-structure (porosity and pore size distribution), SEM micro-structure, nitrogen gas permeation performance. In addition, mechanical and thermal properties were preliminarily investigated. This work aims to develop low-cost porous mineral-based mullite materials in harmony with a strong emphasis on the environment (not only the utilization of waste fly ash to reduce environmental pollution, but also the environmental separation application of the as-prepared porous mullite materials).

2. Experimental procedure

2.1. Starting materials

In the current work, industrial waste fly ash and natural bauxite were used as the starting materials in order to prepare porous mineral-based mullite membrane supports. Fly ash was obtained from Hefei No. 2 thermal power plant (Hefei, Anhui Province, PR China). Natural bauxite mineral was purchased from Yangquan city (Shanxi Province, PR China).

The mixture of fly ash and bauxite, based on the composition of 3:2 mullite ($W_{\text{fly ash}}:W_{\text{bauxite}} = 45.87:100$), was wet-mixed for 12 h with water as medium using polyurethane-coated steel balls in a polyethylene pot. The average particle diameters (d_{50} value) of fly ash, bauxite and their mixture are 1.76, 1.13 and 1.52 μm , respectively. For the mixture powder, most of the particles centered between 1.00 and 4.00 μm in diameter.

The chemical composition and crystalline phase analysis of these two starting materials was described in our precious work [24].

2.2. Pressing and sintering

After wet-mixing for 12 h, the mixture slurry of fly ash and bauxite based on the composition of 3:2 mullite was completely dried at 100 °C. Afterwards, the mixture was slightly crushed to break the agglomerates, mixed with organic binder PVA-1750 (5.00 wt.% solution) and then uniaxially pressed at a pressure of 160 MPa. Both rectangular bars (50 mm \times 6 mm \times 3–4 mm) and cylindrical pellets (25 mm in diameter; 2–3 mm in height) were made in two different

moulds (Zhenjiang Juguang Precision Instruments Processing Co., Ltd.).

After sufficient drying, the samples were fired at various temperatures for 2 h at an interval of 50 °C. Firing was carried out in an electric furnace and the heating rate was 1 °C min⁻¹ up to 450 °C, 2 °C min⁻¹ up to 650 °C, and 2 °C min⁻¹ up to final temperature. A holding time of 1 h was carried out at 450 and 650 °C, respectively, in order to remove added organic additives and inherent structural water in bauxite.

2.3. Characterization techniques

The particle size distributions of fly ash, bauxite and their mixture were determined using a laser particle size analyzer (Rise-2006, Jinan Rise Science & Technology Co. Ltd., PR China) using PEG-10000 (polyethylene glycol; molecular weight: 10,000 g mol⁻¹) as organic dispersing agent.

The sintered samples were directly characterized using XRD (D8 ADVANCE, Bruker Corporation, Germany; Cu K α radiation). The sintering shrinkage behavior of the green rectangular bar (the mixture of bauxite and fly ash based on 3:2 mullite) was measured between room temperature (26 °C) and 1580 °C in a horizontal dilatometer (DIL 402C, Netzsch, Germany). A constant heating rate of 3 °C min⁻¹ was used. The length change was recorded with a dense α -alumina as reference sample.

Micro-structures of the sintered bodies were observed using FE-SEM (field emission scanning electronic microscope; JSM-6700F, JEOL, Japan) after sputtering gold coating on cross-sectional surfaces. The shrinkage percents in diameter direction of the sintered cylindrical pellets were measured using a vernier caliper. In addition, bulk density and open porosity were measured in water medium, respectively, using a conventional method according to the Archimedes' principle.

Pore size distributions were examined in a home-made equipment according to the bubble point method, which is on the basis of gas–liquid replacement mechanism [25]. Also, nitrogen permeation fluxes at different pressures were tested using the dried samples in this experimental device.

Thermal expansion co-efficient of the sintered samples was measured in the above horizontal dilatometer from room temperature to 1000 °C at a heating rate of 10 °C min⁻¹. Room temperature flexural strength was determined by the three-point bending method in a universal materials testing machine (3369, Instron Corporation, USA). A span length of 30 mm and crosshead speed of 0.5 mm min⁻¹ were used. All the tested bars were polished by 360 mesh and then 800 mesh metallographic sandpapers. Fracture strength was calculated according to the following expression (ISO9693 1999).

$$\sigma = \frac{3P \times l}{2b \times h^2}$$

where σ is the fracture strength (Pa), P is the fracture load (N), l is the span length (m), b is the width of samples (m), and h is the height of samples (m).

3. Results and discussion

3.1. Phase evolution mechanism and sintering characteristic

3.1.1. XRD analysis

Fig. 1 shows the XRD result for the mixture of fly ash and bauxite (based on 3:2 mullite), fired at 1200–1500 °C for 2 h. The result proves that the phase compositions of the porous mineral-based mullite depend on thermal treating temperature to a large extent. At 1200 °C, cristobalite was detected because of the phase transition of quartz in two starting materials, i.e., waste fly ash and

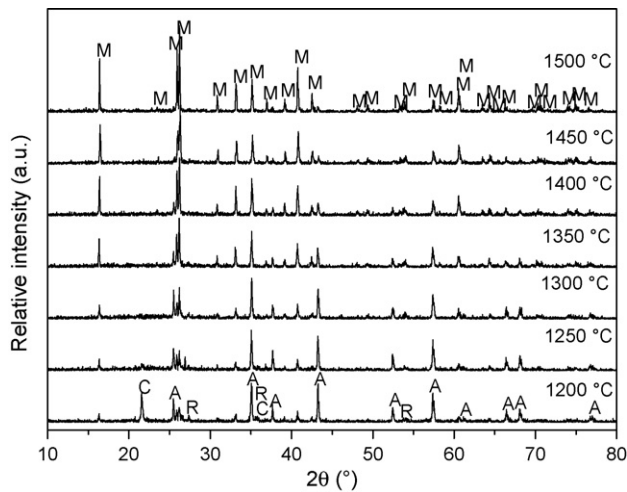


Fig. 1. XRD patterns of the mixture samples sintered at various temperatures for 2 h. Crystalline phase: M, mullite; A, corundum; C, cristobalite; R, rutile.

bauxite. The formation of corundum phase is ascribed to the thermal transition of diasporite in raw bauxite. Also, the weak diffraction peaks of mullite and rutile are observed. The peak intensity of cristobalite dramatically decreases between 1200 and 1250 °C, and then approaches to zero completely at 1300 °C, whereas that of mullite increases gradually from 1200 to 1300 °C. This indicates that corundum, derived from decomposed diasporite, reacted with cristobalite for secondary mullitization by solid state reaction. This phenomenon, generally called secondary mullitization, is usually observed during high-temperature reaction in the kaolin-based mullite [7,9].

From 1300 to 1450 °C, the peak intensity of corundum phase gradually decreases, and almost approaches to zero at 1450 °C because it dissolved into transitory liquid glassy phase for further secondary mullitization. Above 1450 °C mullite is the only crystalline phase present in the sample. For higher firing temperatures, the peaks of mullite become more intense because more mullite crystals precipitated from liquid glassy phase and then grew [26,27].

3.1.2. Sintering shrinkage characteristic

Dilatometric study, carried out on the dry-pressed green bar, displays the sintering shrinkage behavior of the mixture sample based on 3:2 mullite. Fig. 2 illustrates the length shrinkage percent (dL/L_0) and differential length shrinkage percent (dL/dt) as a

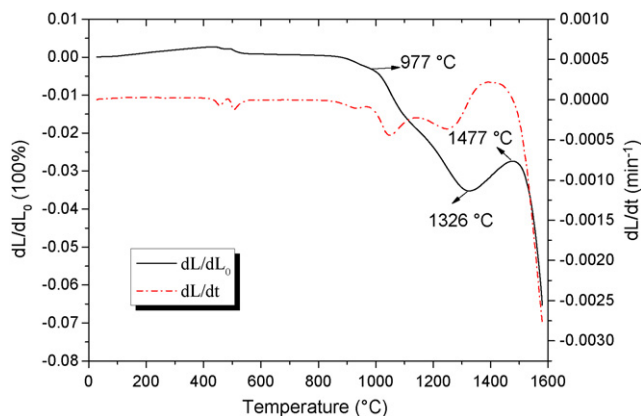


Fig. 2. Linear shrinkage percent (dL/dL_0) and differential linear shrinkage percent (dL/dt) between room temperature and 1580 °C of the mixture sample of bauxite and fly ash based on the composition of 3:2 mullite.

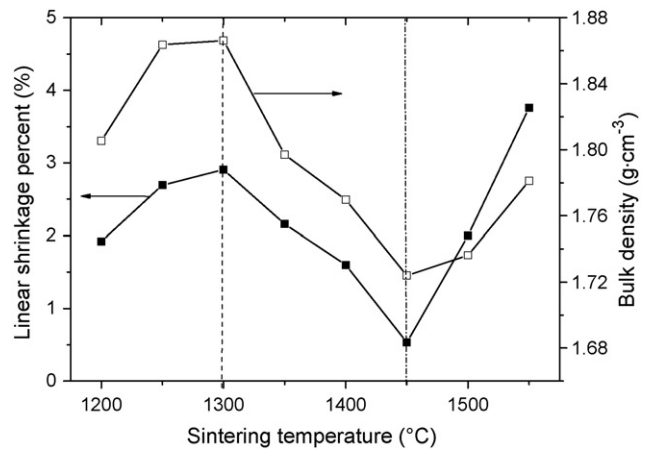


Fig. 3. Linear shrinkage percents and bulk densities of the porous mineral-based mullite membrane supports sintered at different temperatures from 1200 to 1550 °C for 2 h.

function of temperature. At high temperatures, the sintering could be divided into three stages. The sample shrunk significantly from 977 °C. The first stage of densification starts at 977 °C, and extends to 1326 °C. Then, a unique self-expansion stage is observed from 1326 to 1477 °C. The secondary mullitization was accompanied with a volume expansion, while sintering via liquid glassy phase promoted the dimension shrinkage of samples [28]. At this stage, the secondary mullitization reaction predominated the volume change of the sample than the sintering via liquid glassy phase. As mentioned in Section 3.1.1, the mullitization reaction underwent two processes. One is the solid state reaction between corundum and cristobalite, and the other is the dissolution of corundum followed by the precipitation of mullite crystals during the further mullitization. Combined with the sintering behavior analysis, it is concluded that this volume expansion was mainly caused by the further mullitization via the dissolution of corundum followed by the precipitation of mullite.

Above 1477 °C, the sintering entered into the third stage (1477–1580 °C). During this stage, the sample shrunk again as a result of the sintering promotion action of liquid glassy phase. Also, the mullitization reaction completed on the whole. In this case, the influence of glassy phase through sintering on the densification is dominant.

In order to verify the influence of this self-expansion sintering on micro-structural variations, bulk density, SEM, porosity, pore size distribution and nitrogen gas flux were studied in detail.

3.2. Shrinkage percent and bulk density

Fig. 3 displays the sintering shrinkage percents and bulk densities of the sintered porous mineral-based mullite samples. From 1200 to 1300 °C, both linear shrinkage percent and bulk density gradually increase, indicating the enhanced densification of the samples. The decrease in both linear shrinkage percent and bulk density between 1300 and 1450 °C suggests again that this unique volume expansion occurred during high-temperature sintering. With increasing sintering temperature further (from 1450 to 1550 °C), the samples exhibited a characteristic of relatively quick densification. This can be verified by the quick increase in both linear shrinkage percent and bulk density.

3.3. Open porosity and pore size distribution

3.3.1. Open porosity

The open porosities of the porous mineral-based mullite ceramic membrane supports are shown in Fig. 4 as a function of sinter-

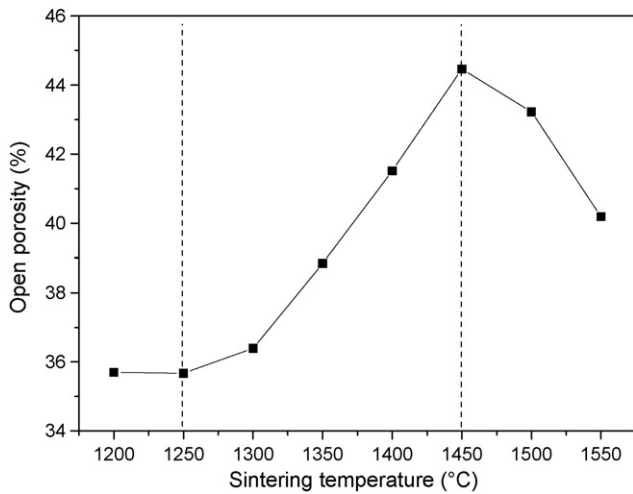


Fig. 4. Open porosities of the mineral-based mullite bodies as a function of sintering temperature between 1200 and 1550 °C.

ing temperature. As can be seen from this figure, porosity first decreases between 1200 and 1250 °C, but increases gradually in the temperature range of 1250–1450 °C, and then decreases again with temperature increasing from 1450 to 1550 °C. During sintering at 1250–1450 °C, the mass of the sample kept unchanged, while the volume increased abnormally. Therefore, at elevated temperatures this increase trend of open porosity was resulted from the above-mentioned sintering self-expansion. This is obviously different from the decreased trend in porosity for porous mullite derived from the kaoline–alumina system [7,8,29], though the mechanism of mullitization is similar each other. At 1450–1550 °C, the samples show a characteristic of decreased open porosity at elevated sintering temperatures. Among these samples sintered at 1200–1550 °C, the maximum open porosity is 44.46% at a sintering temperature of 1450 °C, and the minimum open porosity is 35.67% at a sintering temperature of 1250 °C.

3.3.2. Pore size distribution

Fig. 5 illustrates the pore size distributions (a), and maximum pore diameter and average pore diameter values (b) of the porous mineral-based mullite samples sintered at various temperatures (from 1200 to 1550 °C). As can be seen from the figure, from 1200 to 1250 °C the pores distribution curves slightly shift to the direction of small pore, and both maximum pore diameter and average pore diameter decrease a little. This can attribute to the minor densification at the first sintering stage. From 1250 to 1500 °C, the pore size gradually increases, and the pore size distributions broaden at the same time. The average pore diameters are 0.93, 1.03, 1.25, 1.80, and 2.20 μm for the sintering temperatures at 1300, 1350, 1400, 1450, and 1500 °C. When sintering temperature is increased from 1500 to 1550 °C, the pore size distribution curve broadens, but shifts to the direction of small pore. Correspondingly, the average pore diameter decreases from 2.20 to 2.06 μm, though the maximum pore diameter increases from 4.81 to 5.25 μm.

3.3.3. SEM observation

Fig. 6 shows the cross-sectional micrographs of the porous mineral-based mullite samples sintered at different temperatures for 2 h. It is found that the micro-structures are extremely related to sintering temperature. At 1200 °C, the mixture particles contacted each other compactly, and no significant sintering took place. With sintering temperature increasing from 1300 to 1450 °C, the samples exhibit a more and more porous micro-structure. At the same time, the particles combined each other because of their sintering, which

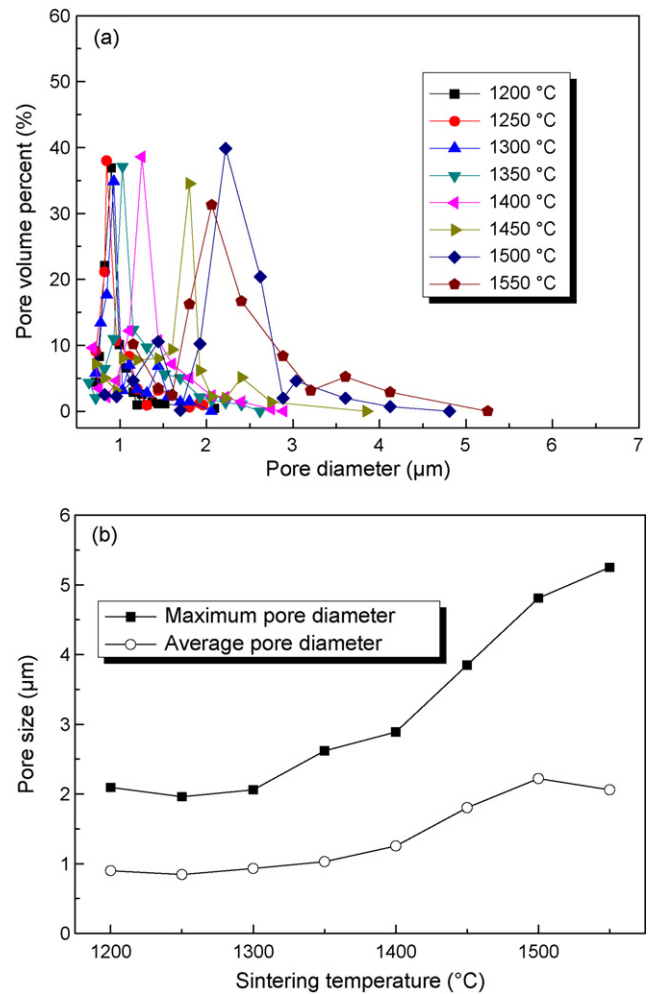


Fig. 5. Pore size distributions (a), and maximum pore diameter and average pore diameter (b) of the porous mineral-based mullite membrane supports sintered at various temperatures in the range of 1200–1550 °C.

resulted in the formation of larger sintered particles. This characteristic is very typical for the samples sintered at high temperatures such as 1450 and 1500 °C. By comparing Fig. 6e with Fig. 6f, it is concluded that at 1500 °C the sample became much denser. Also, no isolated sintered particles are observed, indicating that the relatively significant densification occurred during sintering. This result is consistent with the open porosity result in Section 3.3.1.

3.4. Nitrogen gas flux

Fig. 7 displays the nitrogen gas fluxes under various applied pressures of the porous mullite-based membrane supports sintered at different temperatures. From 1200 to 1250 °C, the nitrogen gas flux slightly decreases at all the applied trans-membrane pressures. The nitrogen gas permeation flux gradually increases from 1250 to 1500 °C, and then dramatically decreases from 1500 to 1550 °C. At 1250–1450 °C, the increase in pore size, combined with the increase in open porosity, results in this increase trend in gas permeation flux. At 1450–1500 °C, the nitrogen gas flux still increases, though open porosity decreases a little (from 44.46% to 43.26%). When a gas flows through porous materials dominated by the viscous flow regime, according to the Hagen–Poiseuille equation [30], gas flux is proportional to both open porosity and the square of pore size. Therefore, the increase in pore size is more beneficial to increase gas flux than the one in open porosity.

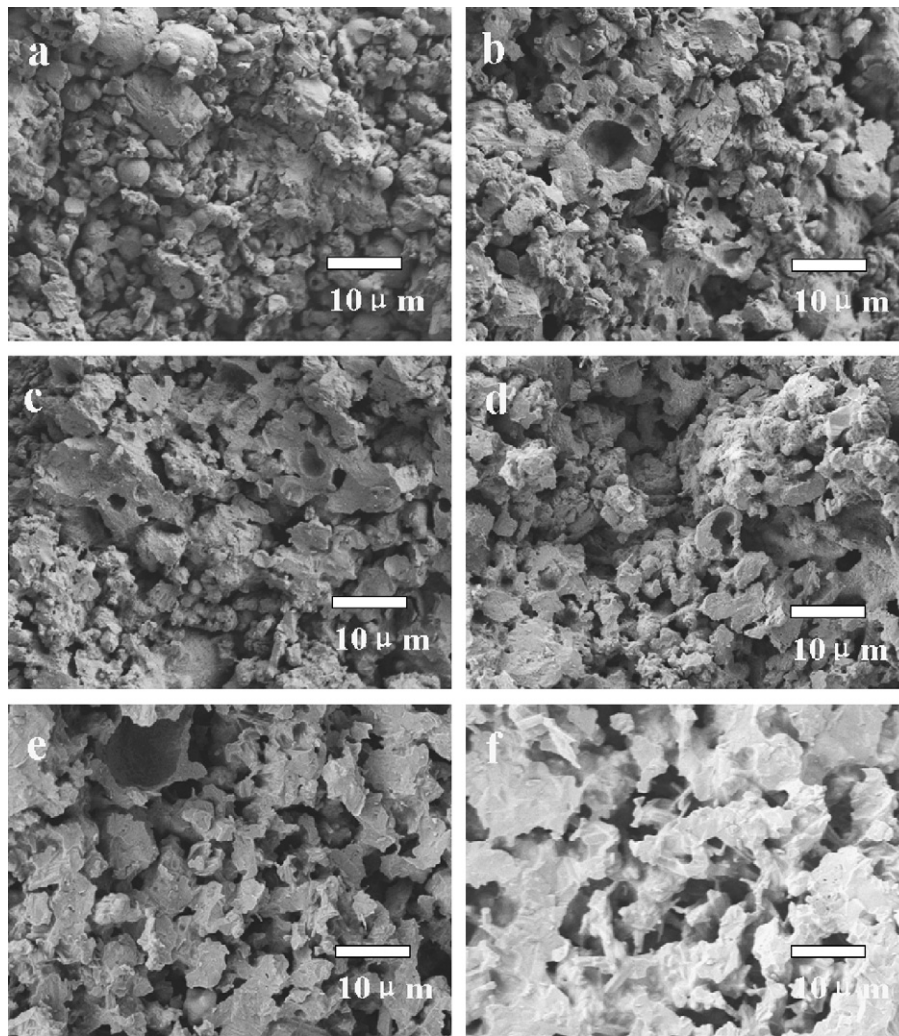


Fig. 6. Cross-sectional SEM microphotographs of the porous mineral-based mullite samples sintered at different temperatures for 2 h: (a) 1200 °C, (b) 1300 °C, (c) 1350 °C, (d) 1400 °C, (e) 1450 °C, and (f) 1500 °C.

At standard atmosphere (0.1 MPa), the maximum nitrogen gas flux is $2.61 \times 10^3 \text{ m}^3 \text{ m}^{-2} \text{ h}^{-1}$, which corresponds to the sample sintered at 1500 °C for 2 h. For the sample sintered at 1500 °C for 2 h, the nitrogen flux slightly decreases under all the applied trans-membrane pressures.

3.5. Thermal and mechanical properties

Fig. 8 presents the thermal expansion co-efficient values of the porous mineral-based mullite membrane supports after sintering at various temperatures for 2 h. Basically, the thermal expansion co-efficient decreases with increasing sintering temperature. From 1250 to 1350 °C, the expansion co-efficient decreases from 7.35×10^{-6} to $6.13 \times 10^{-6} \text{ K}^{-1}$. From 1350 to 1550 °C, the expansion co-efficient decreases very slightly, which varies in the range of $5.85\text{--}6.10 \times 10^{-6} \text{ K}^{-1}$. Although the porosity varies dramatically from 1350 to 1550 °C, the change of thermal expansion co-efficient is quite little, suggesting that all the gas pores relatively uniformly dispersed in the prepared porous mineral-based mullite supports. The similar result has been achieved during the fabrication of porous cordierite supports in our previous work [31]. Compared the theoretic value ($4.5\text{--}5.6 \times 10^{-6} \text{ K}^{-1}$ between 20 and 1000 °C), these comparatively large thermal expansion co-efficient values are mainly due to the existence of other compositions such as silica-rich

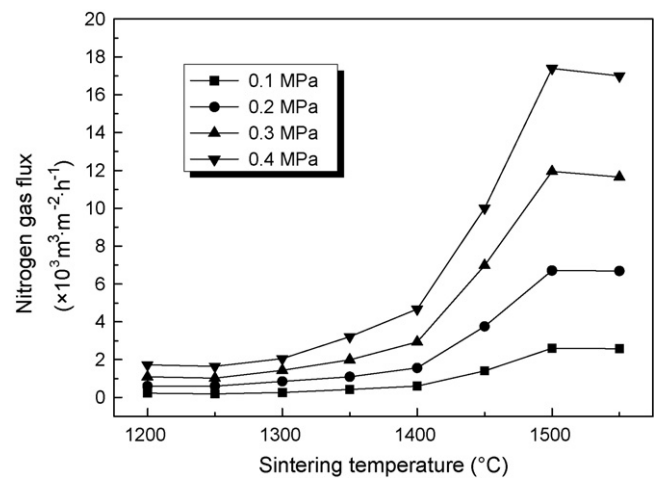


Fig. 7. The variation in nitrogen gas fluxes with different applied trans-membrane pressures of the porous mineral-based mullite supports after sintering at various temperatures for 2 h.

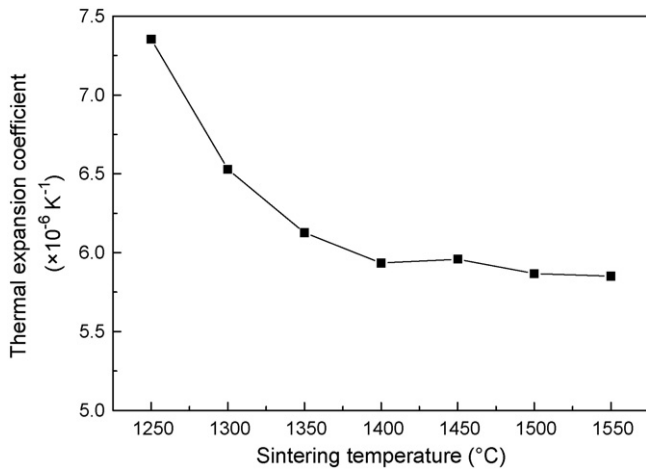


Fig. 8. Linear thermal expansion co-efficient of the sintered porous mullite ceramic membrane supports as a function of sintering temperature in the range of 1250–1550 °C with a holding time of 2 h.

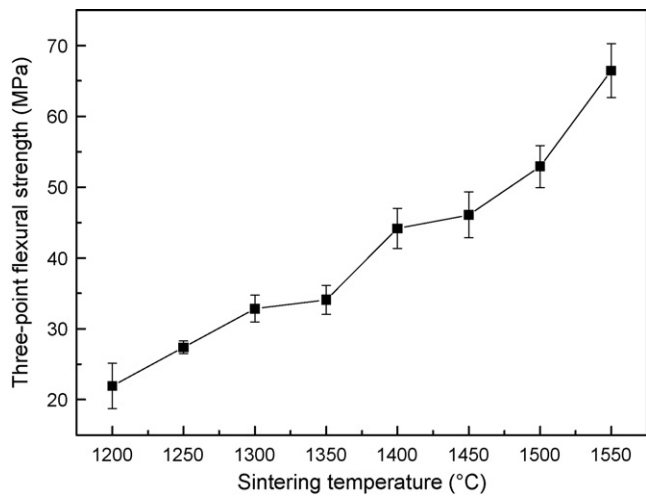


Fig. 9. The variation in flexural strength with sintering temperature (1200–1550 °C) of the sintered porous mullite supports.

glassy phase, alkaline and alkaline-earth metal oxides (Na_2O , K_2O , MgO , CaO , etc.).

Fig. 9 shows the average flexural strength of the porous mullite supports as a function of sintering temperature. Interestingly, the average flexural strength continuously increases at elevated temperatures from 1200 to 1550 °C, though the porosity varies with different sintering temperatures (three temperature zones: 1200–1250; 1250–1450; 1450–1550 °C). At 1200–1250 °C and 1450–1550 °C, accompanied with the decrease in porosity, the increase in flexural strength is well understood because of the occurrence of sintering densification. But at 1250–1450 °C, the average flexural strength increases, though the porosity increases from 35.67% to 44.46%. From the SEM analysis in Section 3.3.3, at elevated temperatures the formation of larger sintered particles through the sufficient sintering between small mixture particles, resulting in the increase of bonding area. In addition, the increase in sintering temperature caused the precipitation and growth of more mullite crystals, which improved mechanical strength. Therefore, the mechanical strength increases at increased open porosity in the temperature range of 1250–1450 °C.

4. Conclusions

Porous mineral-based mullite ceramic membrane supports were prepared directly using the mixture of fly ash and bauxite by the reaction sintering technique. An abnormal sintering self-expansion at elevated temperatures occurred between 1326 and 1477 °C. During this temperature range, corundum dissolved into transitory liquid glassy phase to further develop secondary mullitization reaction. This unique self-expansion caused the decrease in both linear shrinkage percent and bulk density between 1300 and 1450 °C. In the temperature range of 1250–1450 °C, both open porosity and pore diameter increase with temperature, indicating an important effect of sintering self-expansion on micro-structure. A more and more porous micro-structure is also obviously observed by SEM. The increase in pore size, accompanied with the increase in open porosity, results in the increase of gas permeation flux from 1250 to 1500 °C. The expansion co-efficient decreases from 7.35 to $6.13 \times 10^{-6} \text{ K}^{-1}$ at 1250–1350 °C, but then slightly varies in the range of 5.85 – $6.10 \times 10^{-6} \text{ K}^{-1}$ at 1350–1550 °C. At elevated temperatures from 1250 to 1450 °C, the average flexural strength increases, while the porosity increases too. This abnormal increase in mechanical strength is ascribed to the precipitation and growth of more mullite crystals, as well as the increase of bonding area between large sintered particles.

Acknowledgements

This work was financially supported by the Ministry of Science and Technology of China for the financial supports (the international cooperation project: contract no. 2009DFB50490; the 973 project: contract no. 2003CB615700). The authors would also like to thank the Public Education Department of Jiangxi Province for financial support (GJJ08509, GJJ08510, and GJJ08511).

The editor and reviewers are gratefully acknowledged for their good advice. We also thank Mr. Lifeng Miao and Mr. Lang Ying (National Engineering Research Center for Domestic and Building Ceramics, JCU) for the assistance in the mechanical strength and SEM measurements.

References

- [1] S. Masmoudi, R. Ben Amar, A. Larbot, H. El Feki, A. Ben Salah, L. Cot, Elaboration of inorganic microfiltration membranes with hydroxyapatite applied to the treatment of wastewater from sea product industry, *J. Membr. Sci.* 247 (2005) 1–9.
- [2] S. Khemakhem, R. Ben Amar, A. Larbot, Synthesis and characterization of a new inorganic ultrafiltration membrane composed entirely of Tunisian natural illite clay, *Desalination* 206 (2007) 210–214.
- [3] S. Khemakhem, A. Larbot, R. Ben Amar, New ceramic microfiltration membranes from Tunisian natural materials: application for the cuttlefish effluents treatment, *Ceram. Int.* 35 (2009) 55–61.
- [4] Z.Y. Deng, T. Fukasawa, M. Ando, G.J. Zhang, T. Ohji, Bulk alumina support with high tolerant strain and its reinforcing mechanisms, *Acta Mater.* 49 (2001) 1939–1946.
- [5] C. Falamaki, M. Naimi, A. Aghaie, Dual behavior of CaCO_3 as a porosifier and sintering aid in the manufacture of alumina membrane/catalyst supports, *J. Eur. Ceram. Soc.* 24 (2004) 3195–3201.
- [6] Y.C. Dong, J. Diwu, X.F. Feng, X.F. Feng, X.Q. Liu, G.Y. Meng, Phase evolution and sintering characteristics of porous mullite ceramics produced from the flyash- $\text{Al}(\text{OH})_3$ coating powders, *J. Alloys Compd.* 460 (2008) 651–657.
- [7] G.L. Chen, H. Qi, W.H. Xing, N.P. Xu, Direct preparation of macroporous mullite supports for membranes by in situ reaction sintering, *J. Membr. Sci.* 318 (2008) 38–44.
- [8] Y.F. Liu, X.Q. Liu, H. Wei, G.Y. Meng, Porous mullite ceramics from national clay produced by gelcasting, *Ceram. Int.* 27 (2001) 1–7.
- [9] S.J. Li, N. Li, Effects of composition and temperature on porosity and pore size distribution of porous ceramics prepared from $\text{Al}(\text{OH})_3$ and kaolinite gangue, *Ceram. Int.* 33 (2007) 551–556.
- [10] S. Masmoudi, A. Larbot, H. El Feki, R. Ben Amar, Elaboration and characterization of apatite based mineral supports for microfiltration and ultrafiltration membranes, *Ceram. Int.* 33 (2007) 337–344.

- [11] F. Bouzerara, A. Harabi, S. Achour, A. Larbot, Porous ceramic supports for membranes prepared from kaolin and dolomite mixtures, *J. Eur. Ceram. Soc.* 26 (2006) 1663–1671.
- [12] H. Schneider, J. Schreuer, B. Hildmann, Structure and properties of mullite—a review, *J. Eur. Ceram. Soc.* 28 (2008) 329–344.
- [13] A. Esharghawi, C. Penot, F. Nardou, Contribution to porous mullite synthesis from clays by adding Al and Mg powders, *J. Eur. Ceram. Soc.* 29 (2009) 31–38.
- [14] M. Asghari, T. Mohammadi, A. Aziznia, M.R. Danayi, S.H. Moosavi, R.F. Alamdari, F. Agand, Preparation and characterization of a thin continuous faujasite membrane on tubular porous mullite support, *Desalination* 220 (2008) 65–71.
- [15] Y. He, W.M. Cheng, H.S. Cai, Characterization of α -cordierite glass–ceramics from fly ash, *J. Hazard. Mater.* 120 (2005) 265–269.
- [16] S. Kumar, K.K. Singh, P. Ramachandrarao, Synthesis of cordierite from fly ash and its refractory properties, *J. Mater. Sci.* 19 (2000) 1263–1265.
- [17] H. Shao, K.M. Liang, F. Zhou, G.L. Wang, F. Peng, Characterization of cordierite-based glass–ceramics produced from fly ash, *J. Non-Cryst. Solids* 337 (2004) 157–160.
- [18] Y.C. Dong, X.Q. Liu, Q.L. Ma, G.Y. Meng, Preparation of cordierite-based porous ceramic micro-filtration membranes using waste fly ash as the main raw materials, *J. Membr. Sci.* 285 (2006) 173–181.
- [19] J.M.A. Rincàn, M. Romero, A.R. Boccacconi, Microstructural characterisation of a glass and a glass–ceramic obtained from municipal incinerator fly ash, *J. Mater. Sci.* 34 (1999) 4413–4423.
- [20] F. Peng, K.M. Liang, A.M. Hu, Nano-crystal glass–ceramics obtained from high alumina coal fly ash, *Fuel* 84 (2005) 341–346.
- [21] Z. Károlyi, I. Mohai, M. Tóth, F. Wéber, J. Szépvölgyi, Production of glass–ceramics from fly ash using arc plasma, *J. Eur. Ceram. Soc.* 27 (2007) 1721–1725.
- [22] J.M. Kim, H.S. Kim, Processing and properties of a glass–ceramic from coal fly ash from a thermal power plant through an economic process, *J. Eur. Ceram. Soc.* 24 (2004) 2825–2833.
- [23] J.M. Kim, H.S. Kim, Glass–ceramic produced from a municipal waste incinerator fly ash with high Cl content, *J. Eur. Ceram. Soc.* 24 (2004) 2373–2382.
- [24] Y.C. Dong, X.Y. Feng, X.F. Feng, Y.W. Ding, X.Q. Liu, G.Y. Meng, Preparation of low-cost mullite ceramics from natural bauxite and industrial waste fly ash, *J. Alloys Compd.* 460 (2008) 599–606.
- [25] K. Venkataraman, W.T. Choate, E.R. Torre, R.D. Husung, H.R. Batchu, Characterization studies of ceramic membranes. A novel technique using a coulter® Porometer, *J. Membr. Sci.* 39 (1988) 259–271.
- [26] C.Y. Chen, G.S. Lan, W.H. Tuan, Preparation of mullite by the reaction sintering of kaolinite and alumina, *J. Eur. Ceram. Soc.* 20 (2000) 2519–2525.
- [27] M.A. Sainz, F.J. Serrano, J.M. Amigo, J. Bastida, A. Caballero, XRD microstructural analysis of mullites obtained from kaolinite–alumina mixtures, *J. Eur. Ceram. Soc.* 20 (2000) 403–412.
- [28] X.C. Zhong, G.P. Li, Sintering characteristics of Chinese bauxites, *Ceram. Int.* 7 (1981) 65–68.
- [29] Y.F. Liu, X.Q. Liu, S.W. Tao, G.Y. Meng, O. Toff Sorensen, Kinetics of the reactive sintering of kaolinite–aluminum hydroxide extrudate, *Ceram. Int.* 28 (2002) 479–486.
- [30] Z. Wang, Foundation of Separation Technology for Membrane Method, Chemical Industrial Press, Beijing, 2003.
- [31] Y.C. Dong, X.Y. Feng, D.H. Dong, S.L. Wang, J.K. Yang, J.F. Gao, X.Q. Liu, G.Y. Meng, Elaboration and chemical corrosion resistance of tubular macro-porous cordierite ceramic membrane supports, *J. Membr. Sci.* 304 (2007) 65–75.